

Performance-based seismic design of multistory frame structures equipped with crescent-shaped brace

*Original*

Performance-based seismic design of multistory frame structures equipped with crescent-shaped brace / Kammouh, Omar; Silvestri, Stefano; Palermo, Michele; Cimellaro, GIAN PAOLO. - In: STRUCTURAL CONTROL & HEALTH MONITORING. - ISSN 1545-2255. - ELETTRONICO. - 25:2(2018), p. e2079. [10.1002/stc.2079]

*Availability:*

This version is available at: 11583/2679578 since: 2019-08-02T17:44:38Z

*Publisher:*

John Wiley and Sons Ltd

*Published*

DOI:10.1002/stc.2079

*Terms of use:*

This article is made available under terms and conditions as specified in the corresponding bibliographic description in the repository

*Publisher copyright*

(Article begins on next page)

# Performance-based seismic design of multi-storey frame structures equipped with Crescent-Shaped Brace

Omar Kammouh<sup>1</sup>, Stefano Silvestri<sup>2</sup>, Michele Palermo<sup>3</sup>, Gian Paolo Cimellaro<sup>4</sup>,

<sup>1,4</sup> *Department of Structural, Geotechnical & Building Engineering (DISEG), Politecnico di Torino, Corso Duca degli Abruzzi 24, 10129 Torino, Italy*

<sup>2,3</sup> *Department of Civil Engineering, University of Bologna, Italy*

## ABSTRACT

The primary objective of the *Performance-Based Seismic Design* (PBSD) is to provide stipulated seismic performances for building structures. However, a certain degree of design freedom is needed for matching a specific seismic response. This design freedom is not obtainable by the conventional lateral resisting systems because their stiffness and strength are coupled. Here, we put emphasis on the role of the unconventional lateral resisting systems in adding more flexibility to the design. In this paper, we seek to explore the seismic design of moment resisting frame structures equipped with an innovative hysteretic device, known as *Crescent-Shaped Brace* (CSB). One conspicuous feature of this device is its distinctive geometrical configuration, which is responsible for the enhanced nonlinear force-displacement behavior exhibited by the device. A new performance-based approach for the seismic design of the CSB is proposed. The performance of the device is evaluated and its application in multi-storey shear-type structures is investigated. Two case studies were established to illustrate the design methodology. The first is a new two-storey RC structure and the second is an existing three-storey RC structure. Nonlinear time history and pushover analyses are performed to evaluate the behavior of the controlled structures. The analyses show that for each of the two case studies the acceleration-displacement capacity spectrum conforms to the performance objectives curve. This finding confirms the validity of the proposed design approach and the effectiveness of the new hysteretic device in resisting lateral forces.

**Keywords:** *Crescent Shaped Brace, Design method, Dynamic analysis, Performance Based Seismic Design.*

## 1 INTRODUCTION

Recent development in earthquake engineering has resulted in the emergence of new structural design approaches such as the Performance-Based Seismic Design (PBSD) [1]. PBSD is still deemed as a new approach even though its origin can be traced back as far as the late 20th century. The design efficiency of PBSD is the main reason behind its emergence [2]. The Performance-Based Design specifies the main objectives that should be attained by the structure and gives the standards for accepting a specified performance [3]. Today, structures are designed with the goal of achieving a predefined functionality. This is because the challenge is no longer limited to protecting human lives, but extended to minimizing damages and disruption down to reasonable levels. Nevertheless, matching a defined seismic response necessitates additional design freedom that is unable to be achieved by the traditional structural components, such as beams and columns. Here, it is necessary to emphasize the role of the unconventional lateral resisting systems in making the design more flexible and thus allowing to reach specific seismic performances.

<sup>1</sup> Ph.D. student, Politecnico di Torino, email: [omar.kammouh@polito.it](mailto:omar.kammouh@polito.it)

<sup>2</sup> Associate professor, University of Bologna, email: [stefano.silvestri@unibo.it](mailto:stefano.silvestri@unibo.it)

<sup>3</sup> Research Scientist, University of Bologna, email: [michele.palermo7@unibo.it](mailto:michele.palermo7@unibo.it)

<sup>4</sup> Associate professor, Politecnico di Torino, Phone: +39 3386274741, email: [gianpaolo.cimellaro@polito.it](mailto:gianpaolo.cimellaro@polito.it)

Lately, several efforts in the earthquake engineering discipline could find their ways into various advanced lateral resisting systems. These systems can provide enhanced performances to the structure under particular ground motion levels. Examples of such systems include: (a) seismic isolation systems, which disengage the superstructure from its substructure, thereby giving rise to a “conceptual separation between the horizontal and vertical resisting systems” [4]; (b) tuned mass damping systems, which are practically employed to reduce the vibration level of the structure resulted from high lateral excitations [5]; (c) active and semi-active systems, which use the actual seismic vibration to modify the mechanical properties of the structure accordingly [6]; (d) dissipative systems, which are integrated into the superstructure to reduce the damage in the structure through their energy dissipation capability [7]. Whilst the listed systems have been nicely incorporated into practice and literature, none of them could completely fulfil the intended seismic objectives of structures as outlined by the PBSO.

In this paper, we focus on a new innovative lateral resisting device, the *Crescent Shaped Brace* (CSB). CSB is a hysteretic device that is grouped under the ‘energy dissipation devices’ classification. The device enables the structure to have prescribed multiple seismic performances through its passive resisting capability [8]. Up to the present time, the design of multi storey buildings equipped with Crescent Shaped Braces has not been exposed to wide-ranging research. The application of the CSBs is restricted to a single case study of a steel structure in which the braces were inserted at the ground floor. The objective of that study was to obtain a controlled soft-storey response. The upper storeys were braced with conventional concentric steel diagonal braces in order to conceptually model the system as a single degree of freedom (SDOF) system [4].

The work presented in this study proposes a comprehensive method for the seismic design of multi storey shear-type-structures strengthened with CSB devices. In this study, the geometrical and mechanical properties of the controlled structure are assumed to be given, as in the case of existing structures; therefore, there is no control on the structure’s stiffness and strength. This implies that the CSB system is the only variable in the design. In the case of designing new structures, more design freedom is added as the properties of the structure can be chosen in accordance with the desired performance objectives. The design method proposed in the study involves: (i) sizing the CSB devices in the elastic field; (ii) verifying the behavior of the braces in the plastic field. The first part of the method is to design the braces in the elastic field with reference to a predefined performance point. Then, the post yielding behavior of the CSB is determined numerically using the FEM software ‘SeismoStruct V.7.0.6’ [9]. In the second part of the method, the post yielding behavior of the controlled system (i.e. structure equipped with the designed braces) is verified by means of nonlinear pushover and time history analyses.

To illustrate the procedure in all the details, the methodology has been applied to two case study structures. The controlled structures are designed to satisfy the ‘Essential Objectives’ shown in Figure 1 [1]. Non-linear pushover and time-history analyses are performed to verify the performance of the controlled system under a given seismic input. The outcome of the study proved the validity of the proposed design method and the efficiency of the hysteretic device.

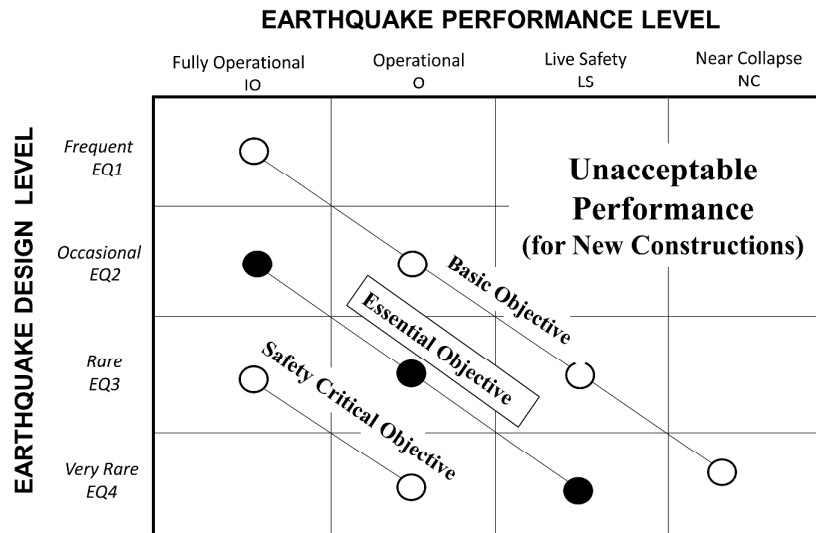


Figure 1. Performance-based seismic design goals. Adopted from [1]

## 2 THE CRESCENT SHAPED BRACES

### 2.1 Overview

The Crescent-Shaped brace (CSB) (Figure 2) is a unique hysteretic lateral resisting device that provides additional design freedom to frame structures. Its geometrical configuration, as shown in Figure 3, permits the structure to have predefined multiple seismic performances [8]. The CSB enables the designer to have full control over the design because its yielding strength and lateral stiffness are not coupled.

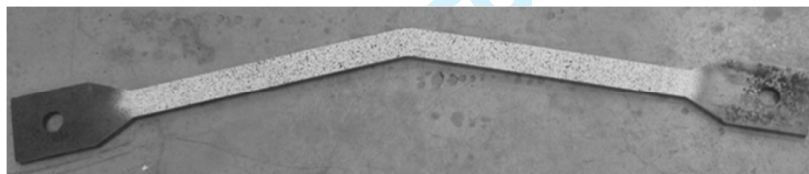


Figure 2. A sample of the Crescent Shaped Brace

### 2.2 Analytic model of the CSB

Previous work conducted on the Crescent-Shaped Braces by Palermo et al. (2015) led to the derivation of analytical formulations for sizing the device based on a target stiffness and a target yielding strength. Eqs. (1) and (2) represent a simplified version of the original equations developed in [8]. The strength and stiffness are initially imposed according to the predefined performance objectives to be achieved. The process involves a consideration of the structural and non-structural responses of the system. Equation (1) allows obtaining the arm ratio of these devices, which is the ratio between the arm of the device  $d$  and the diagonal length  $L$  (see Figure 3). This ratio can be assumed as 0.1 for preliminary designs. The arm ratio is subsequently replaced in Eq. (2) to get the target moment of inertia of the CSB device.

$$\xi = \frac{M_{pl}}{F_y \cdot L} \quad (1)$$

where  $\xi = d / L$  represents the arm ratio of the device,  $d$  is the device arm,  $M_{pl} = W_{pl} \cdot f_y$  is the plastic bending resisting moment of the cross section,  $W_{pl}$  is the plastic section modulus,  $f_y$  is the yield strength,  $\bar{F}_y$  is the target yield strength,  $L$  is the diagonal length (i.e. the line connecting both extremities of the device).

$$J = \frac{L^3 \cdot \bar{K} \cdot \xi^2}{3 \cdot E \cdot \cos^2 \theta} \quad (2)$$

where  $J$  represents the cross-section inertia,  $\bar{K}$  is the target initial lateral stiffness,  $E$  is the modulus of elasticity of the steel section,  $\theta$  is the angle formed between the applied force and the device diagonal (i.e.  $\theta = 0$ ).

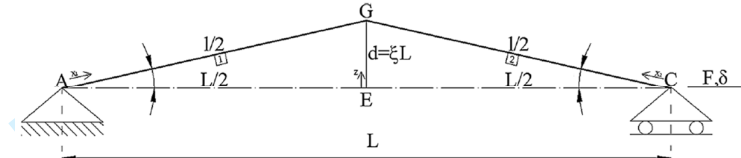


Figure 3. The geometric configuration of the studied device. Adopted from [8]

### 2.3 Mechanical behavior of the CSB

The post-yielding behavior of a random CSB device has been numerically studied using the fiber-based software 'SeismoStruct V.7.0.6', which considers both geometric nonlinearities and material inelasticity. First, a sample of the bracing device 'HEB200 European profile' was subjected to a monotonic rising tension load. The result of the numerical analysis is displayed in Figure 4 (the solid segment of the curve). At the beginning, the CSB responds in flexure, acting linearly until first yielding is reached at the knee section. Then, the device encounters a plastic behavior due to the spread of plasticity (pseudo-horizontal part). This is followed by a second remarkable hardening behavior as the device's arm  $d$  decreases. At this stage, the device mainly reacts through its axial stiffness capacity, like a conventional brace or a truss in a tensile layout.

The same specimen was subjected to a monotonically increasing compressive loading. Figure 4 (the dotted segment of the curve) is a graphical representation of the constitutive law of the device in compression. It is very important to note that unlike traditional concentric braces, the CSB device does not suffer from sudden Eulerian in-plane buckling when exposed to a compressive force, and this is due to its unique shape. Regarding the out-of-plane buckling, the appropriate selection of the cross section is highly effective in preventing such a problem [8] (e.g. choosing balanced inertias along weak and strong axes). Another solution is to include longitudinal ribs in correspondence to the neutral axis fiber.

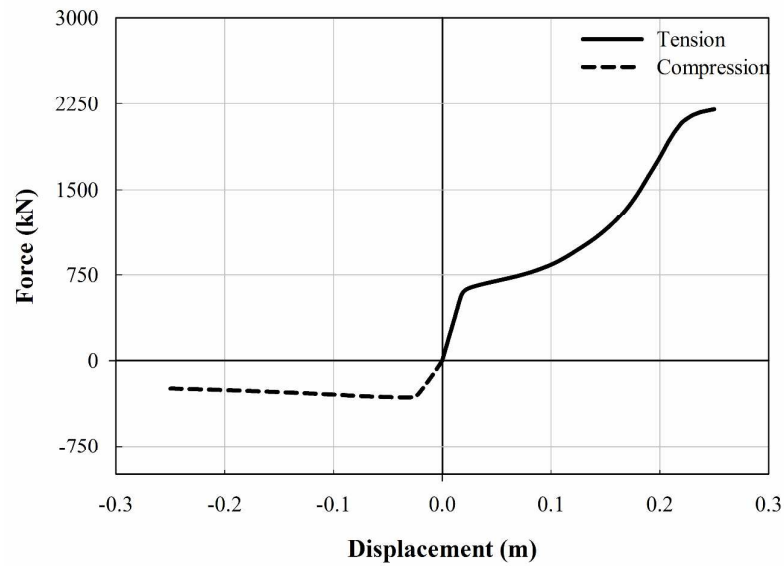


Figure 4. Monotonic behavior of a single CSB in tension and compression

The hysteretic behavior of the CSB is that of typical steel bracings given that the device is nothing more than a steel member having a curved configuration. The numerical studies conducted on the device has demonstrated a good hysteretic response [8]. The simulated hysteretic responses have been also confirmed by experimental tests conducted by some of the authors (the test results will be available soon [10]) and by other researchers [11].

The hysteretic force-displacement response of the single CSB device is strongly asymmetric due to the non-linear geometrical effects [8] [10]: significant hardening response under lateral loads inducing tension in the brace, and softening response under lateral loads inducing compression in the braces (Figure 5a). On the contrary, when two CSB devices are inserted in a two-span frame structure, the overall behavior becomes symmetric, given that one works in compression while the other one works in tension (Figure 5b).

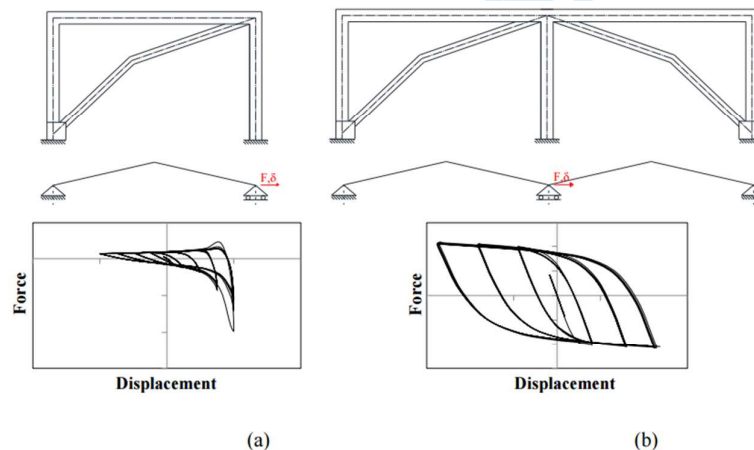


Figure 5. (a) A bilinear CSB device inserted in a frame and its asymmetric force-displacement response; (b) two mirrored disposed bilinear CSB devices inserted in two frames and their symmetric force-displacement response. Adopted from [10].



3 **METHOD: PERFORMANCE-BASED DESIGN OF A MULTI-STOREY SHEAR-TYPE**  
FRAME EQUIPPED WITH CSB DEVICES

The design philosophy behind the use of CSBs as enhanced bracings is grounded on the concept of actively designing a structure behaving according to a so called “Building–Target Capacity (B–TC) curve” that is then translated into a “Building–Actual Capacity (B–AC) curve” [4]. The B–TC curve is the graphical representation of the idealized seismic behavior of the building that we expect to achieve by imposing preselected multiple performance objectives, while the B–AC curve is the graphical representation of the effective seismic behavior of the building, once all structural members are designed. The use of CSBs at all storey levels is the design strategy here adopted to achieve the performance design objectives.

Given that CSBs can be used in different configurations, several design strategies can be identified to achieve the desired performance objectives. In the literature, the behavior of a SDOF steel structure equipped with this device has been investigated [4]. In this section, we propose a general procedure for the seismic design of multi-storey shear-type frame structures equipped with Crescent-Shaped Braces (CSB). The proposed method can be used to design or strengthen structures that do not satisfy particular performance objectives. The design method proposed in the study involves: (i) designing (sizing) the CSB devices in the elastic field; (ii) verifying the behavior of the braces within the global system in the plastic field.

(i) Designing the CSB devices is done with reference to the performance point corresponding to the earthquake level *occasional* (EQ2) and the performance level *fully operational* (IO) (Figure 1). This point belongs to the *Essential Objective* performance line, not the ordinary *Basic Objective* performance line. The reason to choose a high seismic demand is to show the capability of the braces in achieving a predefined performance level. The sizing method comprises 6 steps. In the first step, an initial global stiffness matrix for the controlled structure (i.e. structure equipped with braces) is imposed based on certain criteria, which are described in section 4. The global stiffness matrix is refined as more iterations are executed. In the second step, a modal analysis for the system is performed. The building’s drift obtained from the modal analysis is compared to the design drift that is set according to the desired performance point (i.e. EQ2-IO). The global stiffness matrix is continuously modified through several iterations until the structure’s drift meets the target drift. Once the actual drift matches the design drift, we move to step four and we compute the stiffness of the CSB bracing system. This is done by subtracting the stiffness matrix of the naked structure from the global stiffness matrix. In step five, the structural configuration (i.e. position and number of braces) of the CSB system is defined and hence the stiffness of each brace is computed. Finally, by knowing the stiffness of each device, the moment of inertia and the arm of the devices are evaluated in step 6, and this allows choosing a cross-section for the device from a wide range of cross-sections that satisfy the inertia demand. Once the cross-section is known, the post-yielding behavior of the brace is obtained by means of a static nonlinear pushover analysis using the fiber-based FEM software “SeismoStruct V.7.0.6”. SeismoStruct considers the geometric nonlinearity of the model based on the corotational formula [12], and the material nonlinearity in accordance to Menegotto Pinto law, with adequate focus on the isotropic hardening as given in [13]. The stiffness of the device is computed at each step of analysis, and then updated automatically in the following analysis step. Generally, the post yielding behavior of the device is greatly affected by its section profile; therefore, different section profiles must be compared and the one that conforms most to the predefined performance is chosen.

(ii) The behavior of the CSB system within the global system is obtained by means of nonlinear static pushover (PO) and dynamic time-history (TH) analyses using the FEM software SAP2000 [14]. The behavior of the equipped structure is verified against the performance points ‘EQ3-O’ and ‘EQ4-LS’ shown in Figure 1. The CSB devices are introduced in the model as multi linear links (NL) by importing the force-displacement curves (backbone curves) of the braces obtained from SeismoStruct software. Using the backbone curves of the braces, SAP2000 updates the stiffness of the device at each analysis step according to the displacement exhibited by the

device. The force-displacement curves obtained from SeismoStruct are calibrated in order to account for the structural configuration (inclination) of the devices in the structure. Moreover, the kinematic hysteresis model, which is the default hysteresis model for all metal materials in the program, is considered in the analysis as it is very appropriate for ductile materials. The above mentioned implies that the actual nonlinear stiffness of each device is effectively considered in the analysis. The nonlinearity of the structure is considered using concentrated plastic hinges. The results of both PO and TH analyses are plotted together in order to verify the analysis performed. Finally, the nonlinear pushover curve (i.e. capacity curve) is compared with the predefined performance curve, according to which the devices were initially designed, to check if the target performances are met. Although the nonlinear behavior of the structure equipped with the CSB braces is not designed for 'automatic', previous studies suggested that the system would perform in a good way with respect to severe earthquakes [4] [15] [16] [17]. This is mainly due to the shape of the brace (the peculiar mechanical behavior) (Figure 2) and to its hysteretic dissipation properties. In the following section, we introduce the first part of the methodology (i.e. the design of the CSB system), and in section 5 we cover the second part by means of a case study (i.e. the post yielding verification of the braces within the global system).

#### 4 DESIGN OF THE CSB SYSTEM

The dimensioning procedure of the braces is illustrated in Figure 6. The purpose of this design procedure is to obtain a target lateral stiffness for the single CSB device. The stiffness output is then used in the previously delivered design formulas (Eqs. (1) and (2)) to get the inertia demand of the brace. Once securing the moment of inertia, the cross-section profile of the device can be selected from a broad range of cross-sections. In the following, the design procedure of the CSB is described in all details.

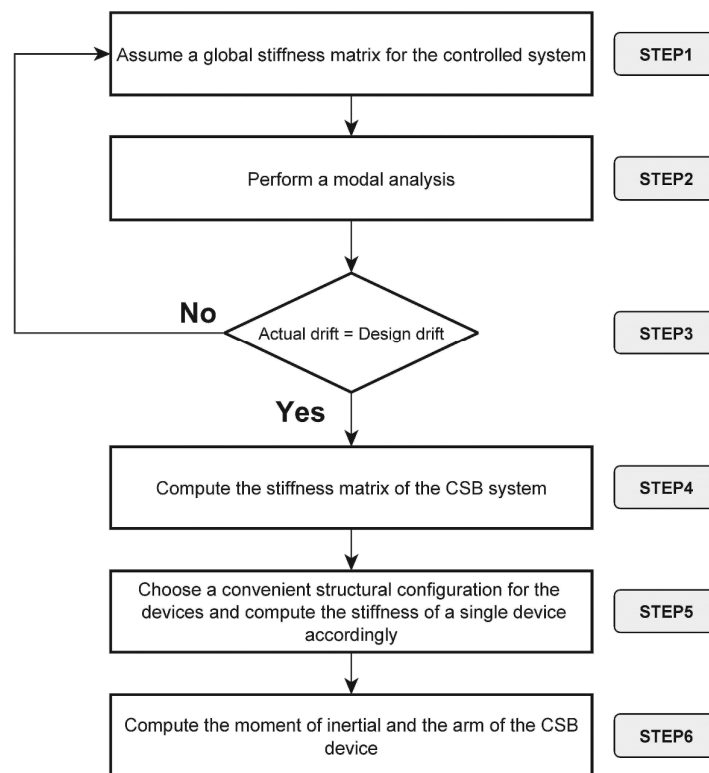




Figure 6. Flowchart of the CSB design scheme

#### 4.1 Step 1: Global stiffness matrix

The global stiffness matrix defines the rigidity of the controlled system. This matrix is determined by summing (as they act in parallel) the stiffness matrices of the bare structure and the bracing system.

$$[K^*] = [K] + [K_b] = \begin{pmatrix} k_1^* + k_2^* & -k_2^* & & & \\ -k_2^* & k_2^* + k_3^* & \ddots & & \\ & \ddots & \ddots & -k_{N-1}^* & \\ & & -k_{N-1}^* & k_{N-1}^* + k_N^* & -k_N^* \\ & & & -k_N^* & k_N^* \end{pmatrix} \quad (3)$$

where  $[K^*]$  denotes the stiffness matrix of the controlled system,  $k_1^*$ ,  $k_2^*$ , ...,  $k_N^*$  represent the stiffness terms of the controlled system at the different storey levels. These stiffness terms are mathematically represented as follows:

$$k_i^* = k_i + k_{bi} \quad (4)$$

where  $k_i^*$  is the stiffness of the controlled system at storey  $i$ ,  $k_i$  is the stiffness of the uncontrolled system at storey  $i$ ,  $k_{bi}$  is the stiffness of the bracing system at storey  $i$ . From the mathematical illustrations above, we see that the global stiffness matrix  $[K^*]$  consists of  $N$  unknowns, denoted as  $k_1^*$ ,  $k_2^*$ , ...,  $k_N^*$ . The number of unknowns, however, can be reduced by enforcing a certain storey-stiffness distribution along the building height. In this work, the storey stiffness distribution is assumed to be proportional to the storey height and mass. The new expressions of the global stiffness matrix components can be obtained using the following formula, where  $m_j$  represents the mass of the  $j^{th}$  storey level,  $z_j$  is the height of the  $j^{th}$  storey level.

$$k_i^* = \frac{\sum_{j=1}^N (z_j \cdot m_j)}{\sum_{j=i}^N (z_j \cdot m_j)} k_1^* \quad (5)$$

The global stiffness matrix can be rewritten in a different form by substituting  $k_1^*$ ,  $k_2^*$ , ...,  $k_N^*$  in Eq. (3). The new global stiffness matrix becomes as follows:

$$[K^*] = \begin{pmatrix} 1 + \frac{\sum_{j=2}^N (z_j \cdot m_j)}{\sum_{j=1}^N (z_j \cdot m_j)} & -\frac{\sum_{j=2}^N (z_j \cdot m_j)}{\sum_{j=1}^N (z_j \cdot m_j)} & & & \\ \frac{\sum_{j=2}^N (z_j \cdot m_j)}{\sum_{j=1}^N (z_j \cdot m_j)} & \frac{\sum_{j=2}^N (z_j \cdot m_j) + \sum_{j=3}^N (z_j \cdot m_j)}{\sum_{j=1}^N (z_j \cdot m_j)} & \ddots & & \\ & \ddots & \ddots & -\frac{\sum_{j=N-1}^N (z_j \cdot m_j)}{\sum_{j=1}^N (z_j \cdot m_j)} & \\ & & & \frac{\sum_{j=N-1}^N (z_j \cdot m_j) + z_N \cdot m_N}{\sum_{j=1}^N (z_j \cdot m_j)} & -\frac{z_N \cdot m_N}{\sum_{j=1}^N (z_j \cdot m_j)} \\ & & & -\frac{z_N \cdot m_N}{\sum_{j=1}^N (z_j \cdot m_j)} & \frac{z_N \cdot m_N}{\sum_{j=1}^N (z_j \cdot m_j)} \end{pmatrix} k_1^* \quad (6)$$

The mathematical illustration in Eq. (6) indicates that the global stiffness matrix is now dependent on just one term ( $k_1^*$ ). For the first iteration, we can set the numerical value of  $k_1^*$  to be the same as  $k_1$ . Alternatively,  $k_1^*$  can be kept as an unknown in the analysis, which makes the method non-iterative. However, modal analyses of systems consisting of more than 3-DOFs would be analytically difficult to deal with if there are many unknowns.

## 4.2 Step 2: Modal analysis

A modal analysis of the controlled system is executed using the initial global stiffness matrix and the mass matrix of the system. The modal analysis enables obtaining the elastic displacements of each respective storey for the different modes. The SRSS rule is then used to combine the elastic displacements, as shown in Eq. (7). Afterwards, we compute the inter-storey drifts for each storey level using Eq.(8).

$$u_i = \sqrt{\sum_{n=1}^N (u_{i,n}^2)} \quad (7)$$

$$\delta_i = |u_i - u_{i-1}| \quad (8)$$

where  $i$  represents the storey number,  $u_i$  is the storey displacement at the  $i^{th}$  storey,  $\delta_i$  denotes the storey drift between two successive storey levels  $i-1$  and  $i$ ,  $n$  is the mode's number,  $N$  is the number of modes.

## 4.3 Step 3: Matching the design drifts

To achieve the predefined design objective, it is essential that the actual and the design inter-storey drifts match. Any discrepancy between the two drifts entails adjustment of the global stiffness matrix. This adjustment is accomplished by adding an increment to the stiffness matrix, as shown in Eq.(9), and then re-running the modal analysis. This increment is illustrated in Eq. (10). It is important to note that either of the global stiffness matrices introduced in Eq. (3) and Eq.(6) can be used in the analysis. Moreover, the designer must verify that the design drift of the structure is less than its yielding drift. This is because we are conducting a linear analysis, and therefore the elastic range should not be exceeded.

$$k_{i,r+1}^* = k_{i,r}^* + C_{i,r} \quad (9)$$

$$C_{i,r} = k_{i,r}^* \cdot \frac{\delta_{i,r} - d_{i,r}}{d_{i,r}} \geq 1 \quad (10)$$

In the above equations,  $r$  represents the iteration step,  $C$  is the modification coefficient,  $\delta$  is the actual drift,  $d$  is the design drift, which is obtained from the predefined performance objective.

## 4.4 Step 4: Stiffness of the CSB system

The target stiffness matrix of the bracing system is acquired by subtracting the stiffness matrix of the uncontrolled structure from the global stiffness matrix, which is obtained in the final iteration of step 3. The mathematical equation is given below:

$$[K_b] = [K^*] - [K] = \begin{pmatrix} k_{b1} + k_{b2} & -k_{b2} & & & \\ -k_{b2} & k_{b2} + k_{b3} & \ddots & & \\ & \ddots & \ddots & -k_{b(N-1)} & \\ & & -k_{b(N-1)} & k_{b(N-1)} + k_{bN} & -k_{bN} \\ & & & -k_{bN} & k_{bN} \end{pmatrix} \quad (11)$$

#### 4.5 Step 5: Stiffness of the single CSB device:

In order to obtain the target stiffness of each CSB device, the target stiffness components of the CSB system ( $k_{b1}, k_{b2}, \dots, k_{bN}$ ) are divided over the total number of devices that exist at the corresponding storey level, as indicated by Eq. (12). It is the sole responsibility of the professional designer to assign the number of devices taking into account the architectural constraints in the building structure.

$$K_{CSB,i} = K_{b,i} / N_{CSB,i} \quad (12)$$

where  $K_{CSB,i}$  represents the stiffness of the single CSB device at the  $i^{th}$  storey,  $N_{CSB,i}$  is the number of devices at the  $i^{th}$  storey.

#### 4.6 Step 6: Moment of inertia of the CSB

At this stage, Eqs. (1) and (2) are used to calculate the moment of inertia of the devices. In these two formulas,  $\bar{K}$  is set equal to  $K_{CSB,i}$ , which is the target stiffness that we seek to achieve, while  $\bar{F}$  represents the target yielding strength at which the device goes inelastic. Once securing a moment of inertia for each CSB unit, a cross-section profile for the CSB is chosen from a broad range of cross sections satisfying the target inertia. It is important to note that the cross-section profile choice may dominate the post yielding behavior of the bracing device. This can have a significant impact on the post yielding behavior of the whole structure [8]. Thus, it is necessary to evaluate different cross-section profiles in order to fulfil the inelastic performance objectives (i.e. performance points corresponding to EQ3-O and EQ4-LS shown in Figure 1).

### 5 POSTYIELDING VERIFICATION OF THE CSB SYSTEM: CASE STUDIES

#### 5.1 The reference structures

The first case study structure (CS1) is a new commercial building situated in Gubbio city, Italy. Gubbio is a city located in the far north-eastern area of the Italian province of Perugia, which is in a comparatively high seismic zone. The building was designed according the Italian seismic standard [18]. Therefore, the building satisfies the operational and the life safety seismic objectives under occasional and rare earthquake levels, respectively. Figure 7 shows the geometry of the building structure. The building is rectangular with dimensions equal to 34.11m x 19.10m. It consists of two storey levels with 4.1m height each. The backbone forming the structure consists of three bays in the y-direction (Elevation 1) and two bays in the x-direction (Elevation 2).

The second case study structure (CS2) is an existing elementary school built in 1983. It is located in Bisignano city, Italy, which is also a high seismic zone. As shown in Figure 8, the building structure has a rectangular planar geometry with dimensions equal to 21.39m x 15.00m. It is made up of three storey levels with a roof pavilion on the top. The backbone forming the structure consists of four bays in the y-direction and three bays in the x-direction. The mechanical properties of the concrete were determined by the presidency of the council of ministers and the department of civil protection in Italy, who performed ultrasonic and rebound hammer tests on a set

of columns and beams. The mechanical and geometrical properties of the concrete elements of both case studies are listed in Table 1.

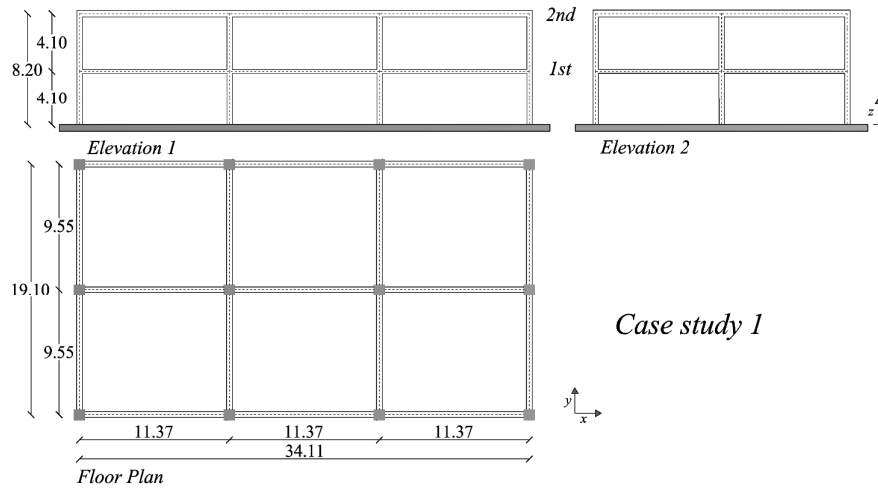


Figure 7. Elevations and plans of the first case study

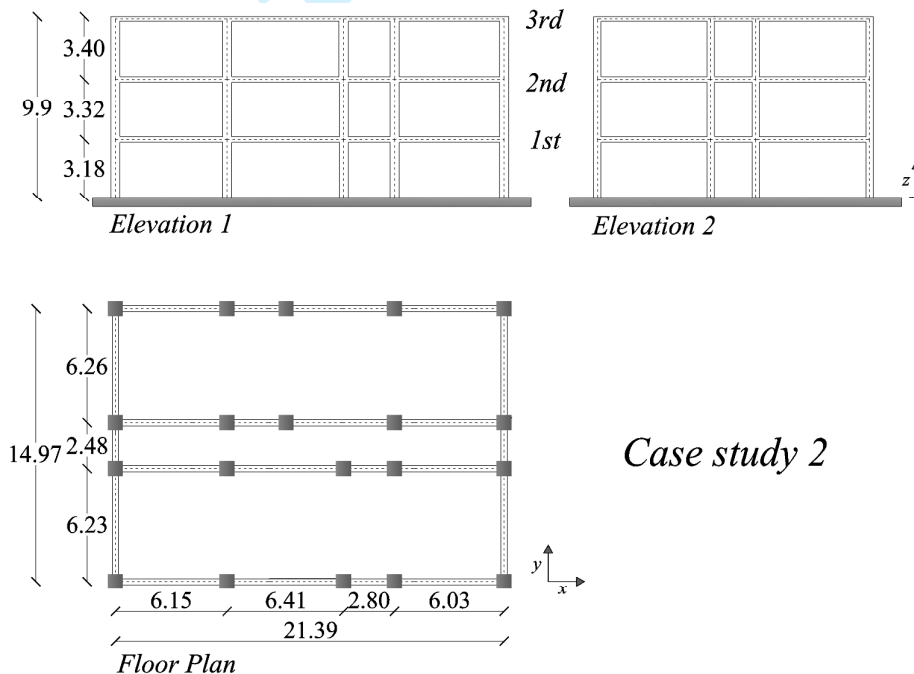


Figure 8. Elevations and plans of the second case study

Table 1 near here

## 5.2 Types of analysis

Two types of non-linear analysis are performed to verify the performance of the case study structures. A three-dimensional model was built using the commercial software SAP2000 in order to perform the analysis. As recommended by the Italian seismic standard, the loads applied to the structure are: (a) the live loads multiplied by a combination factor ( $\psi_E$ ); (b) the dead loads without

any combination factor. The P-Δ effect was neglected given the small height and the high regularity of the structures. The nonlinear behavior of the frames is modelled using concentrated plastic hinges. Flexural Hinges (type Moment M3) were applied to the beam elements, while flexural hinges (type P-M2-M3) were applied to the columns. The hinge force-deformation relationship, also known as the ‘backbone curve’, is obtained using the concentrated plasticity model indicated by FEMA 356 [19].

After designing the CSB devices as introduced in section 4, the force-displacement curve of each device is obtained using SeismoStruct software by performing a nonlinear static pushover analysis. The Braces are then introduced in the SAP model as multi linear links (NL) by importing the force-displacement curves of the braces. The kinematic hysteresis model is considered in the analysis as it is very appropriate for ductile materials (Figure 9).

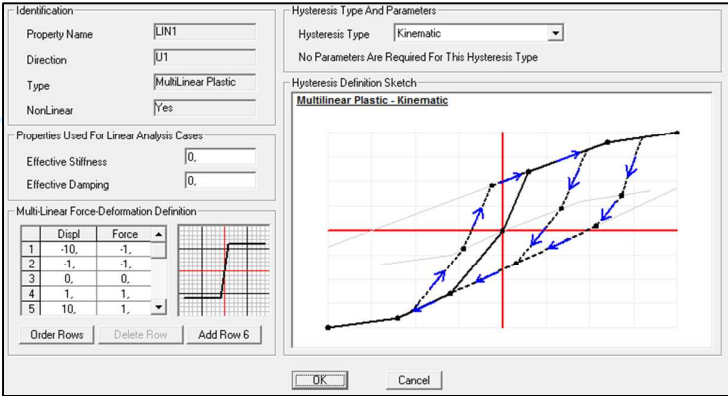


Figure 9. Nonlinear plastic link with kinematic hysteresis type to model the behavior of the CSB in SAP2000.

The first type of analysis is the static pushover analysis, which yields the capacity curve of the structure starting from rest until the failure point [20]. In this analysis, two displacement shapes were applied ‘linear’ and ‘uniform’, whose average is considered. The pushover curve was obtained in terms of the base shear and the roof (top) displacement. The second type of analysis is the dynamic time-history analysis, which was performed using the non-linear direct integration method with a damping ratio of 5%. The analysis was conducted by scaling a set of seven accelerograms to the four design values of PGA at the fundamental period of the structure. The ground motion accelerograms needed for the time-history analysis have been obtained using the software *SIMQKE GR* [21]. The accelerograms are consistent with the design spectra of the structure given by the Italian seismic standard. The Earthquake design levels and the corresponding response spectra parameters are indicated in Table 2. In the table,  $T_y$  represents the return period of the design earthquake,  $PGA$  is the peak ground acceleration,  $F_0$  is the maximum spectral dynamic amplification,  $T_c^*$  is the characteristic period at the beginning of the constant velocity branch of the design spectrum. As shown in the table, the design requirements of the school (CS2) are more stringent than the commercial structure (CS1). The reason is that schools are generally more vulnerable than other types of structures.

Table 2 near here

5.3 Structural configurations and local optimization of the CSB devices

The structural configuration of the bracing devices defines their effectiveness level. A proper arrangement of the bracing devices in the structure would maximize the lateral resistance capacity

while decrease the internal forces in the structural elements. This also leads to a reduction in the devices' cross sections [22]. In addition, high axial force levels can dramatically decrease the moment capacity of columns; therefore, large axial forces should be avoided.

Choosing the right configuration depends on several factors, such as the architectural constraints, the beam span length, and the axial and moment capacities of the columns and foundations. The latter is very important especially if the structure is an existing structure where the structural elements capacities are predetermined. In the design case, on the other hand, the designer can design the columns to stand the additional axial forces coming from the bracing system, and thus this problem can be prevented.

In this section, three possible configurations of the bracing devices (see Figure 10) are investigated by performing a time-history analysis.

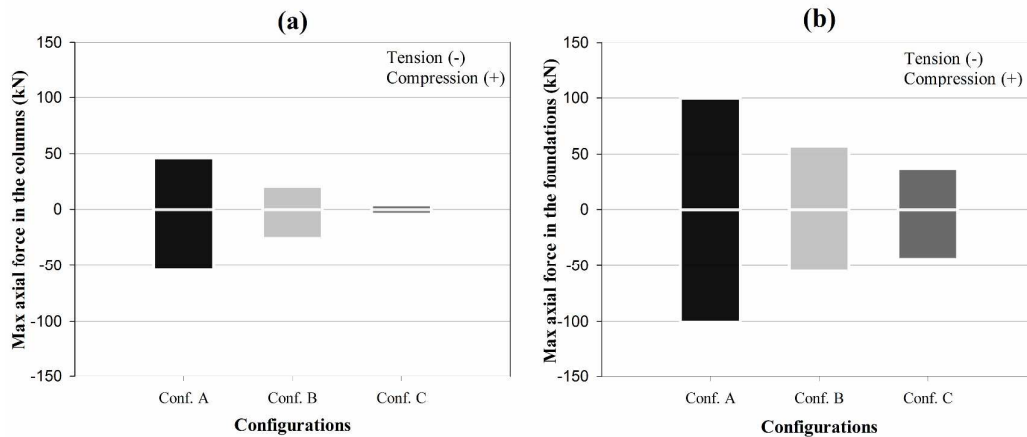


Figure 11 shows the results of the time history analysis in terms of the axial force transmitted into column (C1) and foundation (F1) for each of the configurations. Config. A indicates the highest axial forces in C1 and F1 compared to the other two configurations, whereas Config. B shows small axial forces in columns and foundations. The third configuration Config. C induces almost no axial force in column C1, while it causes the least amount of forces in foundation F1. Among all three configurations, Config. C is the best configuration regarding the internal stresses in columns and foundations; however, this comes at the cost of the resistance efficiency. On the other hand, although Config. A produces the highest amount of forces in the columns and foundations, the resistance efficiency is very high. Finally, Config. B seems to be less problematic in the architectural point of view, as it leaves sufficient area in the façade for windows installation; nevertheless, it is less resistant than the previous two configurations and it causes concentrated stress in the mid span of the beam.

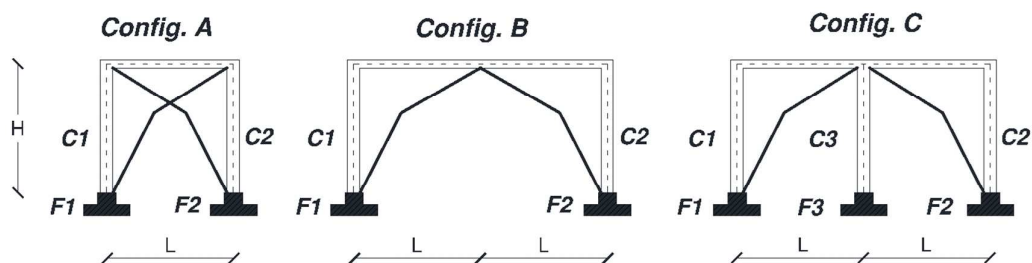


Figure 10. CSB configurations



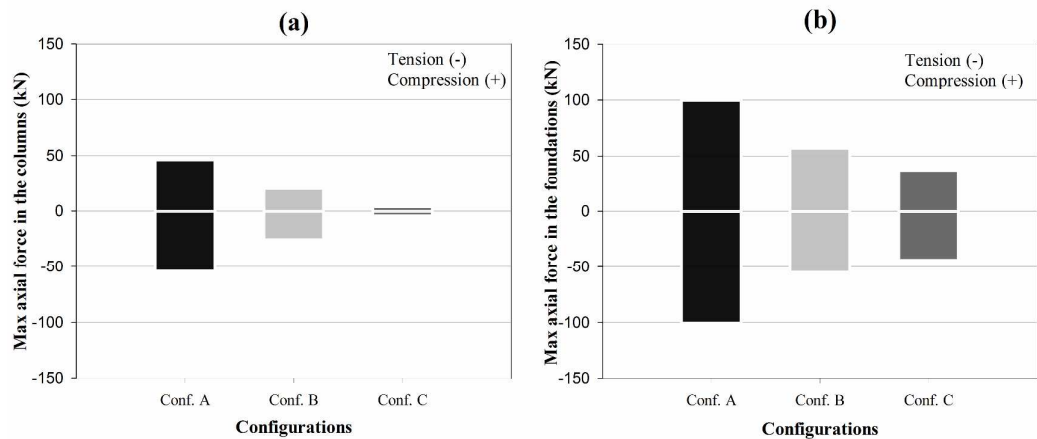


Figure 11. (a) Maximum axial force in column (C1) for each of the three configurations; (b) maximum axial force in foundation (F1) for each of the three configurations

5.4 Performance Objectives

As we mentioned earlier, the first case study (commercial structure) has been designed in compliance with the Italian seismic standard; therefore, the building satisfies the basic design objectives corresponding to the two earthquake design levels ‘occasional’ and ‘rare’ indicated in Figure 1 and Table 2. The second case study (school), on the other hand, is an existing structure; thus, we need first to verify its performance. This is done by performing a pushover analysis to capture the base shear level at which the building yields.

In this work, higher demands are set to be attained by the structures. The *Essential Objectives* specified in Figure 1 are considered instead of the *Basic Objectives* according to which the structures were designed in the first place. The ‘Essential Objectives’ require the structure to remain in a fully operational condition under *occasional* earthquake design level (EQ-2), to stay in an operational condition with limited yielding and damages under *rare* earthquake design level (EQ-3), and to have some degree of damage while preventing life losses under *very rare* earthquake design level (EQ-4).

The Performance Objectives are usually set depending on the client’s requirements, building’s destination, building’s importance, and building’s typology [15]. A study conducted by Bertero et al. established applicable performance limits on the basis of some structural and non-structural damage criteria, such as structural damage indexes (DM), storey drift indexes (IDI), and rate of deformations (floor velocity, acceleration) [1]. Those performance objectives, however, correspond to the *Basic Objectives* (Figure 1); therefore, they cannot be used in our design because our desire is to fulfil higher requirements. Table 3 reveals the basic objectives corresponding to each of the four earthquake levels, as proposed by Bertero et al. (2002). The table also shows two proposed sets of performance limits (for the two case studies) belonging to the *Essential Objectives*. Selecting the new performance limits was done by firstly setting the inter-storey drift index corresponding to EQ-3 (PO-3) to a value that insures no structural or nonstructural damage in the structure. The IDI corresponding to PO-3 of the first case study structure is 0.005 while it is 0.0045 for the second one. The second case study structure was found to yield at a low IDI and this is the reason we set a more stringent performance demand (i.e. IDI=0.0045). Other objective points (PO-1, PO-2, and PO-4) were set proportionally to the corresponding values of PGA at the fundamental period of the structure.

Table 3 near here

## 5.5 Design of the CSB device in the x-direction

Following the CSB design methodology presented in section 4, Table 4 shows the methodology applied to the two case study structures. The reason of considering two case studies is to show the stability of the design method when applied to structures with different occupancies and different seismic demands. Another reason is to stress that existing structures do not always satisfy the seismic standards. For instance, the second case study structure (existing school) yielded at an inter-storey drift index of 0.0045 (PO-3), which does not comply with the Italian seismic standard that requires the building to yield at a higher drift ratio.

Table 4 near here

## 5.6 Numerical verification

In this section, the fulfilment of the pre-defined seismic performance objectives is verified. This was done through a numerical simulation of the seismic behavior of the two case studies. With this purpose, a finite element model for each case study has been developed using SAP2000. The fiber-based software “SeismoStruct V.7.0.6” was used to obtain the constitutive laws of the designed CSB bracing elements, which were then imported to SAP2000 as non-linear links (NL).

First, a non-linear pushover analysis was conducted using two displacement shapes (linear and uniform), whose average was considered. The base shear and the roof (top) displacement were used to signify the force and displacement respectively. Figure 12 and Figure 13 show the capacity spectra of the controlled and uncontrolled structures with their corresponding objective curves in  $S_{ad}$  format for the case studies 1 and 2 respectively. Investigation of the graphs reveals that for each of the two case studies the capacity spectrum (i.e. pushover curve) of the *controlled* structure matches the corresponding predefined target curve (i.e. objective curve). On the other hand, the capacity spectrum of the *uncontrolled* structure was not able to match the corresponding objective curve.

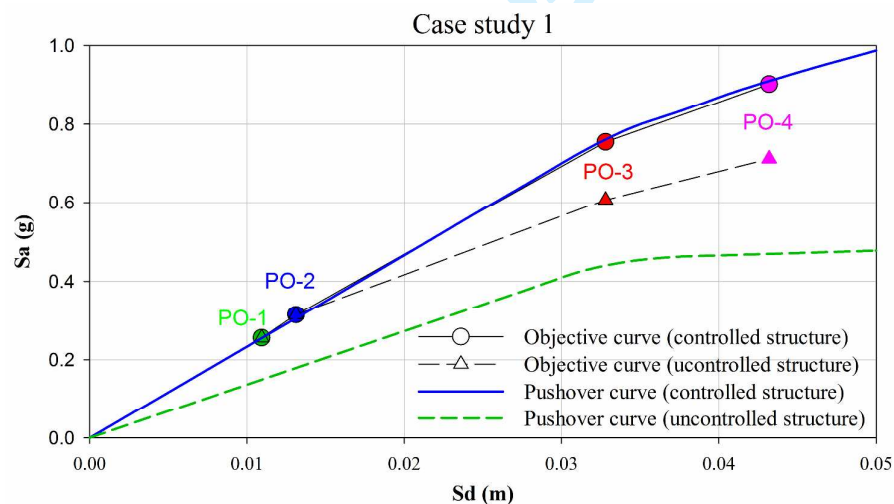


Figure 12. The performance objectives and the results of the pushover analyses in  $S_{ad}$  format of the controlled and uncontrolled structures (Case study 1)

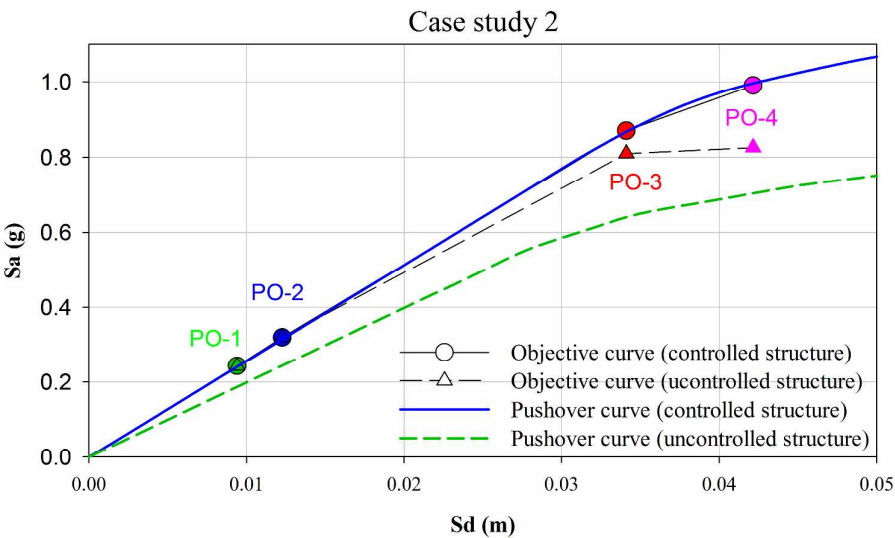


Figure 13. The performance objectives and the results of the pushover analyses in  $S_{ad}$  format of the controlled and uncontrolled structures (case study 2)

Another type of analysis, nonlinear time-history, was performed to assess the seismic performance of the structure. Four groups of spectrum-compatible accelerograms were considered in agreement with the EQ levels reported in Table 2. Each group consists of seven ground motion records scaled to the PGA of the corresponding EQ level at the fundamental period of the structure. The results of the time-history analyses for the two case studies are plotted in Figure 14 and Figure 15 respectively, where each point represents the maximum base shear and ultimate displacement of the corresponding time-history analysis. Investigation of the graph allows observing that the seismic response of the uncontrolled structure fails to achieve the predefined performances, unlike the controlled structure whose time-history analyses results show a large agreement with the prescribed objectives.

It is important to note that the nonlinear behavior of the structure equipped with the CSB braces is not designed for in this study ‘automatic’; however, this good behavior is expected due to the shape of the brace (the peculiar mechanical behavior) (Figure 2) and to its hysteretic dissipation properties, and this is verified in this study.

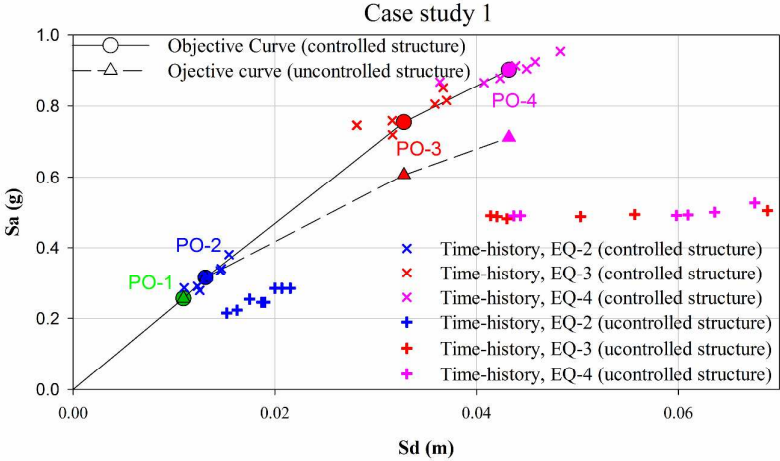


Figure 14. The performance objectives and the results of the time-history analyses in  $S_{ad}$  format of the controlled and uncontrolled structures (case study 1)

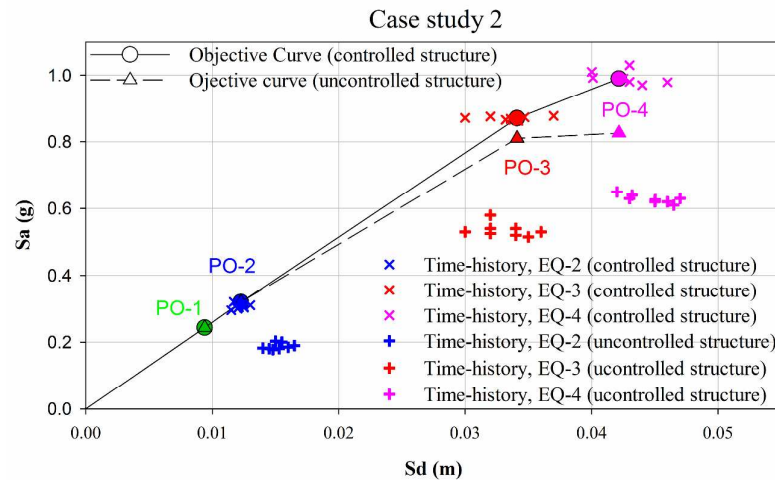


Figure 15. The performance objectives and the results of the time-history analyses in  $S_{ad}$  format of the controlled and uncontrolled structures (case study 2)

## 6 CONCLUSION

In this paper, a comprehensive procedure for the seismic design of multi-storey frame structures equipped with an energy dissipation device “Crescent Shaped Brace” is proposed. The procedure falls within the Performance-Based Seismic Design (PBSD) approach. The first part of the method is to design the braces in the elastic field with reference to the performance point IO-EQ2. Then, the post yielding behavior of the CSB is determined numerically using the FEM software SeismoStruct. In the second part of the method, the post yielding behavior of the controlled system (i.e. structure equipped with the designed braces) is verified by means of nonlinear pushover and time history analyses.

The validity of the method was determined by analyzing two reinforced concrete frame structures equipped with crescent-shaped braces (CSB). First, the performance objectives are chosen. The performance objectives have been expressed in terms of the storey drift index (IDI), which is a measure of the non-structural damage in the structure. Then, the CSB devices have been designed by implementing the proposed design procedure. Static pushover and dynamic time-history analyses were conducted on the case study structures to validate the nonlinear behavior of the CSB within the global system. The analyses performed showed a good behavior of the devices when applied to both case studies although the two structures were of different occupancies and different seismic demands. This confirms the validity of the proposed design approach and the effectiveness of the new hysteretic device in resisting lateral forces regardless of structure’s mechanical properties and the seismic demands.

It is important to point out that all prior efforts to design the CSB were majorly based on SDOF structures. The present design procedure is applicable to both SDOF and MDOF shear-type structures. Future research will be aimed at generalizing the method to be applicable to other types of structures.

## ACKNOWLEDGEMENTS

The research leading to these results has received funding from the European Research Council under the Grant Agreement n° ERC\_IDEal reSCUE\_637842 of the project IDEAL RESCUE— Integrated DDesign and control of Sustainable CommUnities during Emergencies.

Financial supports of Department of Civil Protection (DPC-RELUIS 2014-2018 Grant – Research line 6 "Seismic isolation and dissipation", WP2: "Energy dissipation", Task 2.6: "Definizione di metodi di progetto, procedure e software dedicati ai sistemi di dissipazione di energia e proposte di normativa sviluppate nell'ambito del presente progetto") is gratefully acknowledged.

REFERENCES

[1] R. D. Bertero, V. V. Bertero, Performance-based seismic engineering: the need for a reliable conceptual comprehensive approach. *Earthquake Engineering & Structural Dynamics*, 2002; **31** (3): 627-652.

[2] Özüygür, A. Ruzi, Performance-based Seismic Design of an Irregular Tall Building. *Structures*, 2016; **5**: 112-122.

[3] B. S. Taranath. *Seismic Rehabilitation of Existing Buildings*, Wind and Earthquake Resistant Buildings, CRC Press, 499-584. (2004).

[4] M. Palermo, I. Ricci, S. Gagliardi, S. Silvestri, T. Trombetti, G. Gasparini, Multi-performance seismic design through an enhanced first-storey isolation system. *Engineering Structures*, 2014; **59**: 495-506.

[5] T. Hoang, K. T. Ducharme, Y. Kim, P. Okumus, Structural impact mitigation of bridge piers using tuned mass damper. *Engineering Structures*, 2016; **112**: 287-294.

[6] T. K. Datta. *Seismic Control of Structures*, Seismic Analysis of Structures, John Wiley & Sons, Ltd, 369-449. (2010).

[7] Chopra, K. Anil. *Dynamics of structures: theory and applications to earthquake engineering*, Prentice-Hall, Upper Saddle River, N.J.(2001).

[8] M. Palermo, S. Silvestri, G. Gasparini, T. Trombetti, Crescent shaped braces for the seismic design of building structures. *Materials and Structures*, 2015; **48** (5): 1485-1502.

[9] SeismoStruct. "Seismosoft Earthquake Engineering Software Solutions."

[10] M. Palermo, L. Pieraccini, D. Antoine, S. Silvestri, T. Trombetti, Experimental tests on Crescent Shaped Braces hysteretic devices. *Construction & Building Materials*, (under review).

[11] H. L. Hsu, H. Halim, Improving seismic performance of framed structures with steel curved dampers. *Engineering Structures*, 2017; **130**: 99-111.

[12] A. Correia, F. Virtuoso. (2006), "Nonlinear analysis of space frames." Proceedings of the third European conference on computational mechanics: solids, structures and coupled problems in engineering, C. M. S. e. a. (eds), ed., Lisbon.

[13] F. Filippou, E. Popov, V. Bertero. (1983). "Effects of bond deterioration on hysteretic behavior of reinforced concrete joints." Earthquake Engineering Research Center, University of California, Berkeley.

[14] I. Computers and Structures. (2015), "SAP2000."

[15] I. Ricci, S. Gagliardi, G. Gasparini, S. Silvestri, T. Trombetti, M. Palermo. First-Storey Isolation Concept for Multi-Performance Seismic Design of Steel Buildings. *15 WCEE,2012, LISBOA*.

[16] O. Kammouh, S. Silvestri, M. Palermo, G. P. Cimellaro. (2016), "Application of Crescent-Shaped Brace passive resisting system as a retrofitting system in existing multi-storey frame structures." 1st International Conference on Natural Hazards & Infrastructure ICONHIC2016, Chania, Greece.

[17] O. Kammouh, S. Silvestri, M. Palermo, G. P. Cimellaro. (2016), "Application of Crescent-Shaped Brace passive resisting system in multi-storey frame structures." 6th European Conference on Structural Control, Sheffield, England.

[18] NTC, Norme Tecniche per le Costruzioni, Italian building code, adopted with D.M. 14/01/2008, published on S.O. no. 30 G.U. no. 29 04/02/2008. 2008.



- 1  
2 607 [19] FEMA. (2000). "Seismic Rehabilitation Guidelines."  
3 608 [20] T. K. Datta. *Inelastic Seismic Response of Structures*, Seismic Analysis of Structures, John  
4 609 Wiley & Sons, Ltd, 237-274. (2010).  
5 610 [21] E. H. Vanmarcke, C. A. Cornell, D. A. Gasparini, S. Hou. (1990), "SIMQKE\_GR".  
6 611 [22] X. Yu, T. Ji, T. Zheng, Relationships between internal forces, bracing patterns and lateral  
7 612 stiffnesses of a simple frame. *Engineering Structures*, 2015; **89**: 147-161.  
8 613  
9 614  
10  
11  
12  
13  
14  
15  
16  
17  
18  
19  
20  
21  
22  
23  
24  
25  
26  
27  
28  
29  
30  
31  
32  
33  
34  
35  
36  
37  
38  
39  
40  
41  
42  
43  
44  
45  
46  
47  
48  
49  
50  
51  
52  
53  
54  
55  
56  
57  
58  
59  
60



Table 1. Mechanical and geometrical properties of the structural elements

Characteristics	CS1 (commercial building)	CS2 (school)
Concrete average cubic strength, $R_{ck}$	C45/55, $R_{ck}=55$ Mpa	C20/25, $R_{ck}=24.6$ MPa
Steel yield strength, $f_y$	B540C, $f_y=450$ Mpa	FeB38K, $f_y=375$ Mpa
Modulus of elasticity, $E$	$E=36000$ Mpa	$E=25150$ Mpa
Columns cross-sections	1 <sup>st</sup> level 60cmx60xm 2 <sup>nd</sup> level 50cmx50cm	1 <sup>st</sup> level 50cmx40cm 2 <sup>nd</sup> level 50cmx40cm 3 <sup>rd</sup> level 50cmx40cm
Beams cross-sections	x-direction 50cmx40cm y-direction 50cmx40cm	x-direction 60cmx40cm y-direction 50cmx40cm

Table 2. Earthquake design levels with corresponding response spectra parameters for the two case studies

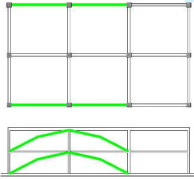
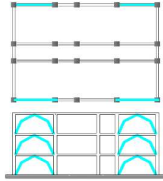
Earthquake design level	Earthquake performance level	$T_r$ [years]		$PGA$ [g]		$F_0$		$T_c^*$ [s]	
		CS1	CS2	CS1	CS2	CS1	CS2	CS1	CS2
EQ1: frequent	Fully operational-IO	30	45	0.071	0.089	2.39	2.27	0.27	0.29
EQ2: occasional	Damage-O	50	75	0.093	0.116	2.34	2.28	0.27	0.32
EQ3: rare	Life safety-LS	475	712	0.230	0.323	2.39	2.45	0.31	0.38
EQ4: very rare	Near collapse-NC	975	1462	0.293	0.426	1.27	2.49	0.32	0.41

Table 3. Quantification of the Basic and the Essential performance objectives

Limit state (Basic objectives)	IDI [1] (Basic objectives)	Limit state (Essential objectives)	IDI (Essential objectives) CS1	IDI (Essential objectives) CS2
EQ1: Fully operational	0.003	EQ1: Fully operational	PO-1 = 0.0015	PO-1 = 0.0013
EQ2: Damage	0.006	EQ2: Fully operational	PO-2 = 0.0020	PO-2 = 0.0018
EQ3: Life safety	0.015	EQ3: Damage	PO-3 = 0.0050	PO-3 = 0.0045
EQ4: Near collapse	0.020	EQ4: Life safety	PO-4 = 0.0067	PO-4 = 0.0055

Table 4. Application of the proposed design methodology to the two case studies

First case study:	Second case study:
<i>Step 1: Global stiffness matrix</i>	
<p>❖ Mass matrix:</p> $[M] = \begin{pmatrix} m_1 & 0 \\ 0 & m_2 \end{pmatrix} = \begin{pmatrix} 8781.55 & 0 \\ 0 & 7035.165 \end{pmatrix} (kN)$ <p>❖ Initial stiffness matrix:</p> $[K] = \begin{pmatrix} 338474 + 163230 & -163230 \\ -163230 & 163230 \end{pmatrix} \left( \frac{kN}{m} \right)$ <p>❖ Initial global stiffness matrix for the first iteration:</p> $[K^*] = \begin{pmatrix} 1 + 0.615 & -0.615 \\ -0.615 & 0.615 \end{pmatrix} k_1 \left( \frac{kN}{m} \right)$ <p>For the first iteration: <math>k_1^* = k_1 = 338474</math> kN/m</p>	<p>❖ Mass matrix:</p> $[M] = \begin{pmatrix} m_1 & 0 & 0 \\ 0 & m_2 & 0 \\ 0 & 0 & m_3 \end{pmatrix} = \begin{pmatrix} 3799.5 & 0 & 0 \\ 0 & 3470.1 & 0 \\ 0 & 0 & 3153.08 \end{pmatrix} (kN)$ <p>❖ Initial stiffness matrix:</p> $[K] = \begin{pmatrix} 362800 + 318810 & -318810 & 0 \\ -318810 & 318810 + 189340 & -189340 \\ 0 & -189340 & 189340 \end{pmatrix} \left( \frac{kN}{m} \right)$ <p>❖ Initial global stiffness matrix for the first iteration:</p> $[K^*] = \begin{pmatrix} 1 + 0.942 & -0.942 & 0 \\ -0.942 & 1.396 & -0.454 \\ 0 & -0.454 & 0.454 \end{pmatrix} \cdot k_1^*$ <p>For the first iteration: <math>k_1^* = k_1 = 362800</math> kN/m</p>
<i>Step 2: Modal analysis (LS response spectrum)</i>	

❖ Inter-storey drifts: $\delta_{01} = 2.63cm$ $\delta_{12} = 3.46cm$	❖ Inter-storey drifts: $\delta_{01} = 2.11cm$ $\delta_{12} = 1.90cm$ $\delta_{12} = 1.84cm$
<i>Step 3: Matching the design drifts</i>	
❖ Design drifts: $\delta_{01,d} = 0.005.h = 0.005 * 410 = 2.05cm$ $\delta_{12,d} = 0.005.h = 0.005 * 410 = 2.05cm$ ❖ Global stiffness matrix at the final iteration: $[K^*] = \begin{pmatrix} 826650 & -312290 \\ -312290 & 312290 \end{pmatrix} \left( \frac{kN}{m} \right)$	❖ Design drifts: $\delta_{01,d} = 0.0045.h = 0.0045 * 318 = 1.43cm$ $\delta_{12,d} = 0.0045 * 332 = 1.49cm$ $\delta_{23,d} = 0.0045 * 340 = 1.53cm$ ❖ Global stiffness matrix at the final iteration: $[K^*] = \begin{pmatrix} 923770 & -401980 & 0 \\ -401980 & 631000 & -229020 \\ 0 & -229020 & 229020 \end{pmatrix} \left( \frac{kN}{m} \right)$
<i>Step 4: Stiffness of the CSB system</i>	
❖ Stiffness matrix of the bracing system: $[K_b] = [K^*] - [K] = \begin{pmatrix} 324950 & -149060 \\ -149060 & 149060 \end{pmatrix} \left( \frac{kN}{m} \right)$ $k_{b1} = 175890 \frac{kN}{m}$ $k_{b2} = 149060 \frac{kN}{m}$	❖ Stiffness matrix of the bracing system: $[K_b] = [K^*] - [K] = \begin{pmatrix} 242160 & -83170 & 0 \\ -83170 & 122850 & -39680 \\ 0 & -39680 & 39680 \end{pmatrix} \left( \frac{kN}{m} \right)$ $k_{b1} = 158990 \frac{kN}{m}$ $k_{b2} = 83170 \frac{kN}{m}$ $k_{b3} = 39680 \frac{kN}{m}$
<i>Step 5: Stiffness of the single CSB device</i>	
❖ Structural configuration of the CSB in the commercial building  $N_{CSB,1} = N_{CSB,2} = 4$ $k_{CSB,1} = \frac{175890}{4} = 43972.5 \frac{kN}{m}$ $k_{CSB,2} = \frac{149060}{4} = 37265 \frac{kN}{m}$	❖ Structural configuration of the CSB in the school building  $N_{CSB,1} = N_{CSB,2} = N_{CSB,3} = 8$ $k_{CSB,1} = \frac{158990}{8} = 19873.7 \frac{kN}{m}$ $k_{CSB,2} = \frac{83170}{8} = 10396.2 \frac{kN}{m}$ $k_{CSB,3} = \frac{39680}{8} = 4960 \frac{kN}{m}$
<i>Step 6: Moment of inertia and cross section profile</i>	
❖ Arm ratio: $\xi = 0.1$ ❖ Moments of inertia: $J_1 = 139684.3 cm^4$ $J_2 = 118377 cm^4$ ❖ Cross sections: $CSB_1$ : rect. $48cm \times 15cm$ $CSB_2$ : rect. $45cm \times 15cm$	❖ Arm ratio: $\xi = 0.1$ ❖ Moments of inertia: $J_1 = 5580.3 cm^4$ $J_2 = 3277.8 cm^4$ $J_3 = 1671.5 cm^4$ ❖ Cross sections: $CSB_1$ : rect. $20cm \times 8.4cm$ $CSB_2$ : rect. $18cm \times 6.8cm$ $CSB_3$ : rect. $14cm \times 7.3cm$

625